

Synthesis and Evaluation of Two Positron-Labeled Nitric Oxide Synthase Inhibitors, *S*-[¹¹C]Methylisothiurea and *S*-(2-[¹⁸F]Fluoroethyl)isothiurea, as Potential Positron Emission Tomography Tracers¹

Jian Zhang,^{†,‡} Timothy J. McCarthy,[†] William M. Moore,[§] Mark G. Currie,[§] and Michael J. Welch^{*,†,‡}

Mallinckrodt Institute of Radiology, Washington University Medical School, 510 S. Kingshighway Boulevard, St. Louis, Missouri 63110, Chemistry Department, Washington University, One Brookings Drive, St. Louis, Missouri 63130, and Searle Research & Development, Monsanto Company, St. Louis, Missouri 63167

Received July 5, 1996[®]

In an effort to develop a tracer for probing inducible nitric oxide synthase (iNOS) levels *in vivo* utilizing positron emission tomography, we have synthesized and evaluated two positron-emitting iNOS selective inhibitors: *S*-[¹¹C]methylisothiurea (**1b**) and *S*-(2-[¹⁸F]fluoroethyl)-isothiurea (**3b**). Prior to fluorine-18 labeling, the nonradioactive fluoro derivative *S*-(2-fluoroethyl)isothiurea (**3a**) was prepared and determined to have a 9-fold higher selectivity for iNOS compared to endothelial NOS (eNOS). Radiochemical synthesis of both compounds, in high radiochemical purity and at high specific activity, was accomplished by the *S*-alkylation reaction of labeled precursors (¹¹CH₃I or ¹⁸FCH₂CH₂OTf) with thiourea. An *in vitro* model, J774 macrophage cell line, was used to assess the uptake of radiolabeled iNOS inhibitor in response to iNOS induction at the cellular level. Increased cell uptake of these two labeled compounds at stimulated iNOS levels, as well as blocking under controlled *in vitro* conditions, was observed. Lipophilicity (log *P*_{o/w}), stability, and tissue biodistribution data of both compounds are reported. Serum stability studies indicate that **3b** metabolized much more rapidly compared to the relatively stable **1b** *in vitro* and *in vivo*. Based on *in vitro* cell uptake data, both tracers were further evaluated in lipopolysaccharide (LPS)-pretreated rats. LPS has been reported to induce iNOS protein expression in the liver, lung, heart, and kidney and other tissues. The uptake for LPS-pretreated rats (6 h post-treatment) was significantly increased in the liver, kidney, and heart for **3b** at 10 min and in the liver and lung for **1b** at 30 min. The results suggest that this first generation of radiolabeled inhibitors may be useful for assessing induction of iNOS *in vivo* with PET.

Introduction

In recent years nitric oxide, NO, has been identified as an important and unique mediator of diverse physiological processes.^{2,3} NO generated from endothelial cells plays a critical role in the regulation of blood pressure by controlling the dilation of blood vessels. In activated macrophages, NO acts as a cytostatic and cytotoxic agent and thus is an important part of the host defense system. NO is also thought to act as a messenger molecule in the brain and as a neurotransmitter in the peripheral nervous system.

Endogenous nitric oxide is generated by nitric oxide synthase (NOS) enzymes, which catalyze the oxidation of L-arginine to L-citrulline, producing NO.⁴⁻⁶ The NOS family of enzymes is composed of an inducible and two constitutive forms. The inducible enzyme (iNOS) is induced in cells including activated macrophages, smooth muscle cells, and hepatocytes. iNOS generates large amounts of NO which are sustained over a long period of time after enzyme induction by cytokines or endotoxins. The two constitutive isoforms of NOS that have been elucidated are as follows: the neuronal enzyme (nNOS), found in brain and peripheral nerve cells, and the endothelial enzyme (eNOS), found in vascular

endothelial cells.⁴ Unlike iNOS, both nNOS and eNOS are intermittently activated by transient elevations in intracellular calcium levels leading to calmodulin binding and stimulation of enzyme activity.

Recent studies have shown that overproduction of NO is associated with several pathological states.⁷⁻⁹ Overproduction of NO by iNOS has been implicated in the functional tissue destruction of chronic inflammation, septic shock, vascular dysfunction in diabetes, and transplant rejection. A substrate analog inhibitor, N^G-methyl-L-arginine (L-NMA), has been used both in animal models¹⁰ and in human clinical trials¹¹ to block iNOS-mediated NO synthesis and to treat hypotension associated with septic shock. Since this compound inhibits both the constitutive and inducible NOS enzymes nonselectively, the patient's blood pressure must be continuously monitored during treatment. Compounds which selectively inhibit a particular isoform of NOS would combine increased therapeutic benefit with lower toxicity. Design and development of inhibitors selective for iNOS is currently of considerable interest in pharmaceutical research.

We are interested in developing a radiolabeled enzyme inhibitor for probing iNOS expression *in vivo* utilizing positron emission tomography (PET),¹² a non-invasive imaging technique which permits monitoring of biochemical processes. In PET studies, short-lived positron-emitting radionuclides such as ¹¹C (*t*_{1/2} = 20.4 min) and ¹⁸F (*t*_{1/2} = 109.8 min) are incorporated into biologically active molecules and used as tracers of physiological pathways. Two major approaches have

* Address correspondence to Michael J. Welch at Washington University Medical School, Campus Box 8225. Tel: (314)-362-8436. Fax: (314)-362-8399. E-mail: Welch@mirlink.wustl.edu.

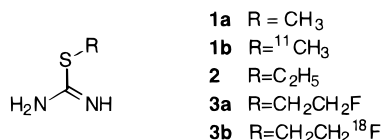
[†] Department of Radiology, Washington University.

[‡] Department of Chemistry, Washington University.

[§] Monsanto Co.

[®] Abstract published in *Advance ACS Abstracts*, December 15, 1996.

Chart 1



been used to probe enzyme activity using PET.¹³ The first includes the use of a labeled substrate whose product is metabolically trapped at the site of catalysis. The second approach involves the use of a labeled enzyme inhibitor bound to the enzyme either covalently or noncovalently with relatively slow dissociation. Several enzymes, including angiotensin-converting enzyme,¹⁴ monoamine oxidase,^{15–17} and dopamine decarboxylase,¹⁸ have been successfully probed with PET using either the radiolabeled inhibitor or the radiolabeled substrate approach. These results have provided valuable information about enzyme activities in normal and diseased states, as well as the effects of novel pharmaceuticals on these enzymatic systems *in vivo*.

PET imaging of a low-capacity enzyme system with labeled inhibitors depends on their target selective uptake and binding affinity. Several stages are involved in developing an effective PET tracer. In general, compounds with high *in vitro* binding affinities and structures suitable for rapid radiolabeling (required by the short half-life of the isotope) are chosen for primary evaluation. Once the target compounds are labeled, their *in vivo* behaviors such as serum stabilities, tissue uptake, and clearance patterns are evaluated. Selection of promising agents is based on high target to nontarget uptake ratios, rapid clearance of nonspecific binding metabolites, and ease of production providing high-specific activity radiopharmaceuticals.¹⁹

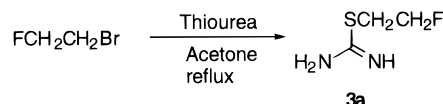
Previous reported work in developing an *in vivo* positron-labeled molecular probe for NOS includes ¹²⁵I-labeled diphenylethylidene bisulfate, which inhibits calmodulin, a cofactor of the constitutive (eNOS and nNOS) enzymes.²⁰ The specificity of this ¹²⁵I-labeled inhibitor in animals, however, was disappointing. Recently, *N*-nitro-L-arginine [¹¹C]methyl ester, an NOS inhibitor, has been precluded for use as a PET tracer due to its instability *in vivo*.²¹

S-Alkylisothioureas (Chart 1) have been reported as potent and competitive NOS inhibitors.^{22–24} These inhibitors have structures which permit incorporation of ¹¹C or ¹⁸F through a simple *S*-alkylation reaction between a labeled alkyl halide (or tosylate) and thiourea. This type of reaction can be completed within the time limits imposed by the short half-lives of the radioisotopes.

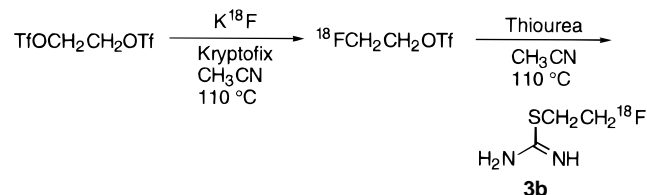
Among known *S*-alkylisothioureas, *S*-ethylisothiourea (**2**, EITU) is 8 times more selective for iNOS over eNOS based on the IC₅₀ reported by Nakane and co-workers.²³ Compound **2** possesses a *K*_i of 5.2 nM for mouse iNOS. Eckelman et al. has suggested that the ratio of enzyme concentration (*B*_{max}) and *K*_i should be at least 4 for an agent to be useful for imaging low-capacity sites with PET.²⁵ For compound **2**, this ratio is about 16, based on a *B*_{max} of 85 nM, estimated from the yield of purified enzyme from lipopolysaccharide (LPS)-treated rat liver.²⁶

Compared to EITU, *S*-methylisothiourea (**1a**) is a less potent and less selective iNOS inhibitor. Compound **1a** was shown to protect rats against circulatory failure and

Scheme 1



Scheme 2



organ dysfunction caused by endotoxins and to increase survival following septic shock in a murine model.²⁷ Compound **1a** was chosen as a second initial target compound for iNOS because it can be directly labeled with ¹¹CH₃I. It provides a comparison in the *in vitro* and *in vivo* studies. Although the model compounds chosen have only moderate selectivity (less selective for iNOS than either aminoguanidine or L-^N^G-(1-iminoethyl)lysine^{28,29} but more selective than *N*^G-methyl-L-arginine), their effectiveness as possible PET tracers is suggested by their higher enzyme affinity (higher inhibitory potency), which should improve target to nontarget uptake.

In this paper, we report the synthesis, characterization, and *in vitro* as well as initial *in vivo* evaluation of two labeled NOS inhibitors for PET, one labeled with carbon-11, *S*-[¹¹C]methylisothiourea (**1b**), and the other with fluorine-18, *S*-(2-[¹⁸F]fluoroethyl)isothiourea (**3b**). Before attempting fluorine-18 labeling, the non-radioactive fluoro derivative *S*-(2-fluoroethyl)isothiourea (**3a**) was prepared, and its inhibitory potency and selectivity for iNOS compared to the parent compound, *S*-ethylisothiourea (**2**), were determined.

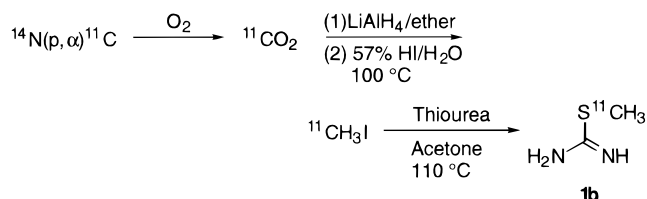
Results and Discussion

Synthesis. Compound **3a** was prepared in a one-step *S*-alkylation reaction by modification of a reported method.³⁰ Under our best conditions, 1-bromo-2-fluoroethane and thiourea in acetone were refluxed overnight to afford a 45.8% yield of **3a** after column purification and recrystallization (Scheme 1).

Compound **3b** was synthesized in a two-step reaction. 1-[¹⁸F]Fluoroethyl trifluoromethanesulfonate ([¹⁸F]fluoroethyl triflate) was produced by nucleophilic displacement of ethylene glycol bistriflate with [¹⁸F]fluoride.³¹ This unstable and highly reactive synthetic precursor reacts with thiourea to provide **3b** in 4.5–10% decay-corrected yield (Scheme 2). The specific activity of **3b** was determined by HPLC to be 120–300 Ci/mmol at the end of synthesis. The variation in specific activity was due to the presence of a coeluting side product, most likely due to the reaction of thiourea with either ethylene glycol bistriflate or 1-[(trifluoromethyl)sulfonyl]ethanol, impurities present in the [¹⁸F]fluoroethyl triflate. Although a number of separation conditions have been tried, we were unable to resolve **3b** from the coeluting side product on the cation exchange column.

[¹⁸F]Fluoroethyl triflate has been previously reported as an alkylating reagent for secondary amines. Others have observed similar low yields when using [¹⁸F]fluoroethyl triflate as an *N*-alkylating agent.^{32,33} The

Scheme 3

**Table 1.** Comparison of IC₅₀ Values for Inhibition of Human NOS Isoforms

compd	IC ₅₀ ^a (μM)		selectivity ^b hiNOS/heNOS
	hiNOS	heNOS	
1a	3	7	2.3
2	0.16	1.3	8
3a	0.14	1.26	9
L-NMA	27	6	0.2

^a IC₅₀ values were determined with hiNOS and heNOS by testing each compound at eight concentrations. ^b Selectivity is defined as the ratio of the IC₅₀(heNOS) to IC₅₀(hiNOS).

specific activities routinely obtained for production of **3b** are suitable for use in PET studies for this enzyme system. At these values, the amount of material administered in both *in vitro* and *in vivo* studies would not saturate the enzyme or perturb the system.

Attempts to improve the yield of **3b** included the use of two other radiolabeled synthetic precursors. However, no desired product was observed over a 2 h time period in various solvents, including acetonitrile, acetone, and DMSO, and at a range of temperatures from ambient to 110 °C when either 1-bromo-2-[¹⁸F]fluoroethane³⁴ or 1-[¹⁸F]fluoroethyl toluenesulfonate^{35,36} was used as the S-alkylating agent.

Compound **1b** was prepared by methylation of thiourea with ¹¹CH₃I and purified by HPLC (Scheme 3). The synthesis and purification were accomplished within 50 min. Incorporation yields were in the range of 50–80% (decay-corrected), and in each case, the radiochemical purity was greater than 99%. The specific activity was 500–800 Ci/mmol at the end of synthesis.

Assay of NOS Activity. NOS activity was measured using a previously described procedure.²⁹ The inhibitory potencies, as well as selectivities, of **3a** were determined using human inducible NOS (hiNOS) and human endothelial NOS (heNOS). Compound **3a** showed a potency similar to its parent compound, S-ethylisothiurea (**2**). Compound **3a** was approximately 9 times more selective for iNOS (0.14 μM) than for eNOS (1.26 μM) (Table 1). S-Methylisothiurea (**1a**) was a less potent and less selective inhibitor compared to either **2** or **3a**.

As mentioned earlier, S-alkylisothiureas have recently been reported by different groups as potent and competitive NOS inhibitors. The IC₅₀ of S-ethylisothiurea, reported by Nakane and co-workers,³⁷ showed a selectivity for iNOS similar to our results. The K_i of this compound reported by Garvey and co-workers²² showed the same trend, with lower selectivity for different isoforms of NOS. Although high selectivity is preferred, the moderate selectivity is acceptable for our purposes due to the greater concentration of iNOS compared to the constitutive form. As an example, Knowels et al. have reported an increase of NOS activity by a factor of 30 in the livers of endotoxin-treated rats compared to controls; basal NOS activity is mainly due to the activity of eNOS and nNOS.³⁸

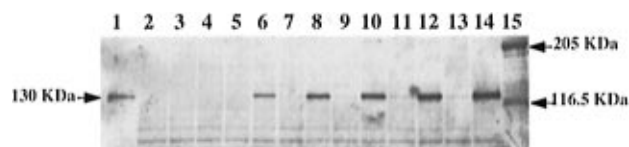


Figure 1. Time course of iNOS expression in the J774 macrophages treated with LPS or with both LPS and γ -interferon (IFN- γ). An anti-iNOS mouse monoclonal antibody was used in the Western blot analysis: lane 1, positive control; lane 2, cells untreated (control); lanes 3, 5, 7, 9, 11, 13, cells treated with LPS for 2, 4, 6, 8, 12, and 24 h, respectively; lanes 4, 6, 8, 10, 12, 14, cells treated with LPS and IFN- γ for 2, 4, 6, 8, 12, and 24 h, respectively; lane 15, molecular weight marker.

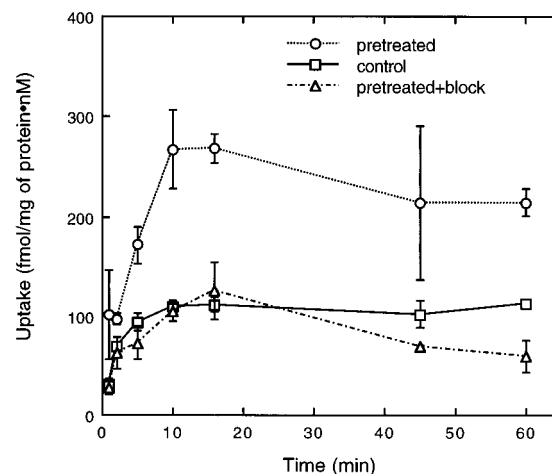


Figure 2. Uptake of **3b** in J774 macrophage cells vs time. Results are expressed as mean \pm SD; $n = 4$.

Partition Coefficients (log $P_{o/w}$). Partition coefficients for **3b** and **1b** were measured by octanol/water extraction at pH 6.8. The partition coefficient was calculated as the average ratio of cpm/g of octanol to cpm/g of water per extraction. Experiments were conducted in quadruplicate. The average log $P_{o/w}$ values of the two back-extractions for the four trials were 0.73 ± 0.03 and -0.04 ± 0.04 for **3b** and **1b**, respectively. The low log $P_{o/w}$ value of compound **1b** will limit its permeability, particularly into the brain.

Cell Studies. To avoid the complication of interanimal variance and interference of metabolites, a murine macrophage cell system (J774 cell line) was used to evaluate uptake of these radiolabeled iNOS inhibitors in response to iNOS induction at the cellular level. iNOS expression in the J774 cell line was induced by treatment with LPS and γ -interferon or with LPS alone.^{39–42} The optimum iNOS induction time and conditions were determined by Western blot using a commercially available iNOS monoclonal antibody. Cells treated with LPS or a combination of LPS and γ -interferon showed increased iNOS levels compared to the control (Figure 1). iNOS upregulation was substantially more significant in the cells treated with both LPS and γ -interferon. iNOS levels reached a maximum at 24 h.

In the tracer uptake experiment, iNOS was induced with Dulbecco's modified Eagle's medium (DMEM) containing LPS and γ -interferon for 24 h in the pretreatment group as well as in the blocking group. The control group was treated with DMEM only for 24 h. The uptake of **3b** and **1b** is presented as $\text{fmol} \cdot (\text{mg of protein})^{-1} \cdot (\text{nM}_0)^{-1}$ in Figures 2 and 3, respectively.

Initial cell uptake of both tracers increased with time. Uptake of **3b** reached a plateau after 10 min; uptake of

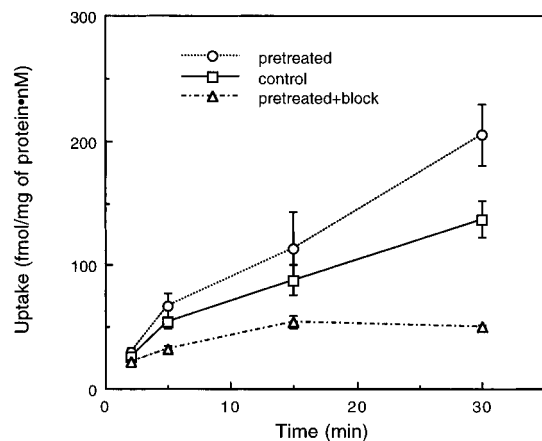


Figure 3. Uptake of **1b** in J774 macrophage cells vs time. Results are expressed as mean \pm SD; $n = 4$.

1b did not reach equilibrium during the duration of the experiment. This time differential may be accounted for by differences in lipophilicity of **3b** and **1b**. Increased uptake was observed for both tracers in both LPS- and γ -interferon-pretreated cells as compared to the control cells. This increased uptake was blocked by incubation with 0.1 mM *S*-ethylisothiourea. In addition, stabilities of both **3b** and **1b** have been checked at the same conditions as the cell uptake experiment.

We observed elevated uptake of these radiolabeled iNOS inhibitors in response to iNOS induction in J774 macrophage cells. This increased uptake and blocking under the controlled *in vitro* conditions indicate the specific uptake of these tracers. Both **3b** and **1b** remained intact during the entire cell uptake process. The *in vitro* data suggested that both **3b** and **1b** may have potential for monitoring increased levels of iNOS *in vivo*.

Recently, increased cell permeability has been observed along with iNOS induction. Enhanced uptake of L-arginine and inhibitors in the J774 cells has been observed over short time frames when iNOS was induced.^{42,43} The authors of those studies hypothesize that treatment of the J774 cells with endotoxin and cytokine results in induction of not only iNOS but also γ^+ transporter protein, which contributed to the enhanced uptake of L-[¹⁴C]-N^G-monomethylarginine. It is suggested that the γ^+ transport system is selective for basic amino acids. Such a system is unlikely to be relevant to the isothiuronium salts, particularly lipophilic compound **3b**.

Serum Stability Study. To determine the biological half-lives of the two compounds *in vivo* and *in vitro*, plasma samples of both tracers were analyzed using SCX HPLC. After 30 min, **3b** was 85% decomposed *in vivo* and 75% decomposed *in vitro*; **1b** was 20% decomposed *in vivo* and 8% decomposed *in vitro*. Detailed stability vs time curves for **3b** and **1b** are shown in Figure 4. The decomposed products were not identified for either **3b** or **1b**. HPLC analysis of both *in vitro* and *in vivo* plasma samples showed similar chromatographic patterns for both **3b** and **1b**; most of the decomposition products eluted at the solvent front on an SCX column.

Stability study results show that compound **3b** is less stable than **1b**. Bone uptake did not fully account for the loss of **3b**, which indicates that defluorination is not the only metabolic route contributing to the instability of the compound. Isothiourea salts are known to react

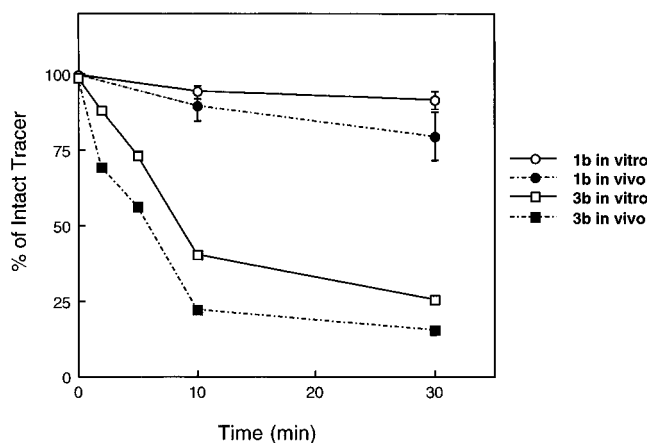


Figure 4. Percent intact **1b** and **3b** remaining in the rat serum *in vivo* and *in vitro* versus time. Data for **3b** are combined from two experiments at different time points (one experiment at 2, 5, and 30 min; the second experiment at 10 min). Data for **1b** are the average of two experiments; the ranges are given.

Table 2. Biodistribution of **3b** in Mature Female Sprague-Dawley Rat^a

organ/ tissue	percent injected dose/g \pm SD, ^b $n = 5$			
	10 min	30 min	1 h	3 h
blood	0.32 \pm 0.03	0.27 \pm 0.02	0.32 \pm 0.05	0.19 \pm 0.02
lung	1.02 \pm 0.12	0.57 \pm 0.06	0.38 \pm 0.01	0.17 \pm 0.01
liver	0.95 \pm 0.03	0.51 \pm 0.08	0.35 \pm 0.02	0.16 \pm 0.02
kidney	1.82 \pm 0.18	1.06 \pm 0.15	0.64 \pm 0.07	0.21 \pm 0.01
muscle	0.33 \pm 0.04	0.38 \pm 0.04	0.32 \pm 0.02	0.14 \pm 0.01
fat	0.08 \pm 0.01	0.07 \pm 0.02	0.07 \pm 0.01	0.04 \pm 0.01
heart	0.62 \pm 0.01	0.37 \pm 0.04	0.29 \pm 0.01	0.16 \pm 0.01
brain	0.14 \pm 0.02	0.15 \pm 0.01	0.17 \pm 0.01	0.16 \pm 0.02
abdominal aorta	0.38 \pm 0.03	0.31 \pm 0.07	0.26 \pm 0.03	0.16 \pm 0.03
bone	0.55 \pm 0.03	0.82 \pm 0.24	0.88 \pm 0.06	1.19 \pm 0.18

^a See the Experimental Section for details. ^b SD is standard deviation.

readily with nucleophiles.⁴⁴ With amines, this leads to the formation of amidines.^{45,46} The lack of stability observed may be associated with the electron-withdrawing group fluorine on the alkyl chain, which could facilitate this nucleophilic displacement. Since the metabolism rate *in vitro* is comparable to that *in vivo*, we speculate that the majority of the metabolism occurs in the blood.

Even though **1b** appeared to have inferior inhibitor potency *in vitro*, its greater stability suggested the worthiness of *in vivo* evaluation. The instability of **3b** led us to investigate shorter time points for biodistribution studies, despite the longer radioactive half-life of fluorine-18.

Biodistribution Studies. *In vivo* biodistribution results of no-carrier-added **3b** and **1b** in mature female Sprague-Dawley rats are presented in Tables 2 and 3, respectively. The injected radioactive dose was approximately 10 and 40 μ Ci/rat for **3b** and **1b**, respectively. Biodistribution data for **3b** shows that activity was retained in the brain during the 3 h experiment. The muscle and the abdominal aorta retained activity for 1 h followed by slow wash out. Biodistribution data of **1b** indicate that activity was retained in the muscle during the 45 min sampling time. The brain uptake of **1b** is very low. Activity associated with **1b** is retained for only 30 min in the abdominal aorta and then washed out gradually. Whether tissue retention of activity was

Table 3. Biodistribution of **1b** in Mature Female Sprague–Dawley Rats^a

organ/tissue	percent injected dose/g \pm SD, ^b n = 4			
	5 min	15 min	30 min	45 min
blood	0.18 \pm 0.04	0.16 \pm 0.04	0.11 \pm 0.01	0.08 \pm 0.00
lung	0.73 \pm 0.02	0.39 \pm 0.01	0.30 \pm 0.02	0.21 \pm 0.02
liver	0.92 \pm 0.12	0.44 \pm 0.06	0.34 \pm 0.02	0.25 \pm 0.01
kidney	3.27 \pm 1.03	1.04 \pm 0.19	0.81 \pm 0.04	0.56 \pm 0.06
muscle	0.18 \pm 0.04	0.20 \pm 0.01	0.23 \pm 0.03	0.21 \pm 0.03
fat	0.06 \pm 0.01	0.02 \pm 0.01	0.02 \pm 0.01	0.03 \pm 0.00
heart	0.72 \pm 0.08	0.30 \pm 0.03	0.22 \pm 0.02	0.17 \pm 0.02
brain	0.05 \pm 0.01	0.04 \pm 0.01	0.03 \pm 0.01	0.02 \pm 0.00
abdominal aorta	0.21 \pm 0.06	0.20 \pm 0.02	0.20 \pm 0.02	0.14 \pm 0.09

^a See the Experimental Section for details. ^b SD is standard deviation.

due to nonspecific binding or to binding of both compounds to cNOS is unknown. Both **3b** and **1b** showed rapid clearance in tissues such as lung, liver, heart, and kidney. High activity found in the kidneys was possibly due to the excretory role of this organ. The increased amount of radioactivity associated with bone samples indicated that some defluorination of **3b** occurred at later time points.

The brain uptake of **1b** is very low, as would be anticipated for a compound of low lipophilicity. The brain uptake of **3b** is slightly less than that of compounds used routinely for neuroimaging,^{47,48} but much greater than the level associated with a nonextracted tracer, where the activity would be about 4% of the blood activity on a percent injected dose per gram basis.⁴⁹ However, it is not known whether the brain uptake of **3b** is associated with the brain or the vascular wall.

Levels of iNOS have been shown to increase in rats when they are treated with endotoxins such as LPS. The LPS-induced iNOS mRNA and protein expression was demonstrated in the liver, lung, spleen, heart, kidney, and brain by Northern hybridization and Western blot analyses.^{26,38,50} Macrophages are reported to be the major site of iNOS expression in endotoxin-treated rats shown by a tissue immunochemical localization study.⁵¹

On the basis of the *in vitro* data, pretreatment studies were performed in rats to determine whether LPS treatment affected the uptake of **3b** or **1b**. The first group ($n = 4$) was pretreated with 10–20 mg/kg LPS, 6 h before tracer injection. The second group ($n = 4$) was left untreated and used as a control. Increased uptake ($p < 0.05$) of **3b** at 10 min was found in the liver, kidney, and heart in the LPS pretreated group as compared to the control (Figure 5a). However, increased uptake of **3b** was not seen at the 30 min time point (Figure 5b). This may be due to rapid metabolism *in vivo*. Enhanced uptake ($p < 0.05$) of **1b**, which was more stable than **3b** both *in vivo* and *in vitro*, was observed in the liver and lung at 30 min in the pretreated rats compared to the control group (Figure 6).

The uptake for LPS-pretreated rats was not significantly increased in the brain for **3b** nor in the heart, kidney, or brain for **1b**. We attribute this to several possible factors including controversy over whether iNOS increases in the brain after LPS treatment (although recent reports showed iNOS mRNA and protein expression in the brain,^{50,51} earlier studies did not detect increased iNOS activity in the brain by measuring citrulline formation³⁸) or the interference of metabolites in our measurements.

We were not able to block the increased uptake of either **3b** or **1b** in the LPS-treated rats using 10–20

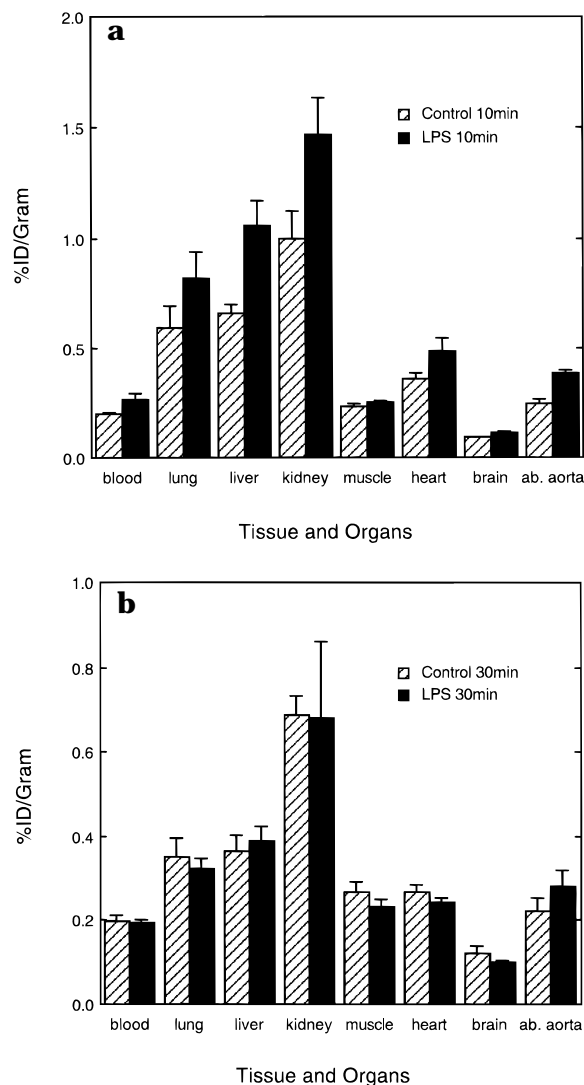


Figure 5. (a) Comparison of tissue biodistribution data for **3b** in LPS-pretreated rats vs control rats at (a) 10 min and (b) 30 min. Mature female Sprague–Dawley rats were used in the experiment; results are presented as average percent injected dose per gram of tissue (%ID/g) \pm SD ($n = 4$). In panel a, the uptake of lung, liver, kidney, heart, and abdominal aorta is statistically significantly ($p < 0.05$) higher in the LPS (10 mg/kg)-pretreated group compared to the control. In panel b, no difference in uptake was observed between the LPS (10 mg/kg)-pretreated group and control group in sampled tissue/organs.

mg/kg of either *S*-methylisothiourea or *S*-ethylisothiourea (data not shown). This may be explained by a pressor effect²⁴ of both compounds at the dose we employed. In the 1940s Smirk and co-workers^{52,53} reported that oral or intravenous administration (hu-

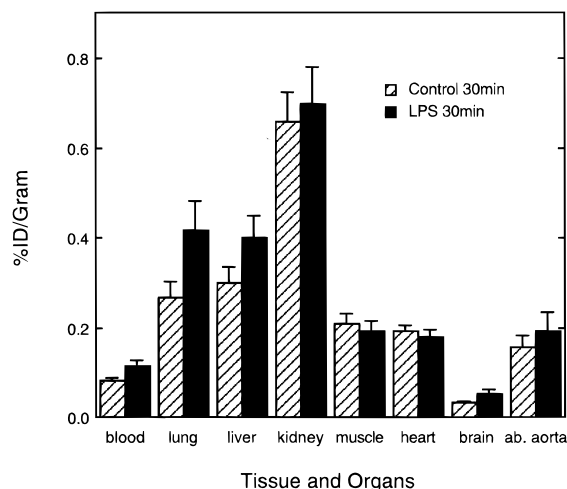


Figure 6. Comparison of tissue biodistribution data of **1b** in LPS-pretreated rats vs control rats at 30 min. Mature female Sprague–Dawley rats were used in the experiment; results are presented as average percent injected dose per gram of tissue (%ID/g) \pm SD ($n = 4$). The uptake of lung and liver is statistically significantly ($p < 0.05$) higher in the LPS (10 mg/kg)-pretreated group compared to the control group.

mans, dogs, and rabbits) of *S*-methyl- and *S*-ethyl isothiourea furnished an immediate rise in blood pressure and respiratory rate for doses as low as 3 mg/kg of body weight. Such a pharmacologic effect would alter the tracer input function. This inability to block tracer uptake *in vivo* means that we have not proved that the increased uptake is due to upregulation of iNOS. However, increased uptake in both *in vitro* and *in vivo* situations, together with the observed blocking in the well-controlled *in vitro* study, is suggestive.

Conclusion

We have developed two positron-emitting iNOS selective inhibitors: *S*-[^{11}C]methylisothiourea (**1b**) and *S*-[2- ^{18}F]fluoroethyl)isothiourea (**3b**). The increased cell uptake at stimulated iNOS levels and blocking under the controlled *in vitro* conditions were observed and suggest that both **3b** and **1b** may have potential for monitoring increased levels of iNOS *in vivo*. As an initial study, an LPS-pretreated rat model with widespread tissue expression of iNOS was used. Enhanced uptake of **3b** and **1b** was observed in some of the organs that are reported to possess increased iNOS levels in LPS-pretreated rats. Further evaluation of these compounds in other animal models with localized iNOS induction in specific tissues is indicated.

Experimental Section

Materials and Methods. Unless otherwise stated all chemicals were obtained from Aldrich Chemical Co. (Milwaukee, WI). Proton and carbon-13 magnetic resonance spectra were obtained on a Varian Gemini 300 spectrometer at 300 and 75.46 MHz, respectively. Fluorine-19 NMR was performed on a Varian 300XL spectrometer at 282 MHz. Proton and carbon-13 NMR chemical shifts are reported in ppm downfield from internal Me_4Si (δ scale). Fluorine-19 NMR chemical shifts are reported in ppm upfield from internal CFCl_3 (ϕ scale). The NMR data are reported in the form: chemical shift (multiplicity, number of protons, coupling constant). All coupling values are in hertz (Hz). Fast atom bombardment (FAB) mass spectra were obtained on a VG ZAB-SE double-focusing mass spectrometer. Elemental analysis was performed by Galbraith Laboratories, Inc. (Knoxville,

TN). HPLC for the radiochemical experiments was performed on a Spectra-Physics 8700 chromatograph equipped with a Whatman Partisil 10 SCX HPLC column, a Waters UV detector (Lambda-Max Model 480, operating at 229 nm), a well-type $\text{NaI}(\text{Tl})$ scintillation detector and associated electronics, and a fraction collector. The HPLC columns used in this work were the following: for the purifications and stability studies of radiolabeled product, a semipreparative column Whatman Partisil 10 SCX (0.9×50 cm), and for the determination of radiochemical purity and specific activity of the radiolabeled product, an analytical SCX column (0.46×25 cm).

Synthesis of 2-(Fluoroethyl)isothiourea Chloride (3a). To a stirred solution of thiourea (0.20 g, 2.63 mmol) in 5 mL of acetone at room temperature was added dropwise 1-bromo-2-fluoroethane (258 μL , 2.89 mmol). The mixture was refluxed overnight under a N_2 atmosphere; then the solvent was removed by rotary evaporation. The residue was dissolved in 1 mL of H_2O and applied to a 10 mL Biorad AG 50W-X8 cation exchange resin (200–400 mesh, H^+ form). The resin was first washed with 20 mL of water and then with 1.0 N HCl. Collected fractions were checked by SCX HPLC, and those containing the desired product were concentrated on the centrifugal evaporation system to give the product as an off-white powder. This powder was further purified by recrystallization (methanol/ether) to afford pure **3a** (0.191 g, 45.8%): ^1H NMR (CD_3OD) δ 4.76 (dt, 2H, $J_{\text{F-C-H}} = 46.5$, $J_{\text{H-C-C-H}} = 5.4$), 3.51 (dt, $J_{\text{F-C-H}} = 25.2$, $J_{\text{H-C-C-H}} = 5.4$); ^{13}C NMR δ 172.45, 82.80 (d, $J_{\text{F-C}} = 169.9$), 32.44 (d, $J_{\text{F-C}} = 21.5$); ^{19}F NMR ϕ -216.955 (tt, $J_{\text{H-C-F}} = 45.78$, $J_{\text{H-C-C-F}} = 24.42$); MS (FAB) 123 (M^+ , 100). Anal. ($\text{C}_3\text{H}_8\text{ClFN}_2\text{S}$) C, H, N.

Assay of NOS Activity. Quantitation of NOS activity was attained by monitoring the conversion of L-[2,3- ^3H]arginine to L-[2,3- ^3H]citrulline. hiNOS and heNOS were purified for use by Monsanto as follows: Enzyme (10 μL) was added to 40 μL of 50 mM Tris (pH 7.6) and the reaction initiated by the addition of 50 μL of a solution containing 50 mM Tris (pH 7.6), 2.0 mg/mL bovine serum albumin, 2.0 mM DTT, 4.0 mM CaCl_2 , 20 μM FAD, 100 μM tetrahydrobiopterin, 2.0 mM NADPH, and 60 μM L-arginine containing 0.9 μCi of L-[2,3- ^3H]arginine. For constitutive NOS, calmodulin was included at a final concentration of 40 nM. Following incubation at 37 $^\circ\text{C}$ for 15 min, the reaction was terminated by addition of 300 μL of ice cold buffer containing 10 mM EGTA, 100 mM HEPES (pH 5.5), and 1.0 mM citrulline. The [^3H]citrulline was separated by chromatography on Dowex 50W X-8 cation exchange resin and radioactivity quantified using a liquid scintillation counter. All assays were performed at least in duplicate with standard deviations of 10% or less. Production of [^3H]citrulline was linear with time over the course of the assay.

Radiochemical Synthesis of [^{18}F]Fluoroethyl)isothiourea Chloride (3b). The synthetic precursor [^{18}F]fluoroethyl triflate was prepared as reported.³¹ [^{18}F]Fluoride was produced by an $^{18}\text{O}(\text{p,n})^{18}\text{F}$ reaction on an enriched oxygen-18 water target.⁵⁴ [^{18}F]Fluoride from the water target was added to a solution of Kryptofix [2.2.2] (6.0 mg, 16.2 μM) and K_2CO_3 (1.5 mg, 10.9 μM) in a 5 mL Vacutainer. Water was azeotropically evaporated using HPLC grade acetonitrile (3×0.5 mL) in a 110 $^\circ\text{C}$ oil bath under a stream of nitrogen. Potassium [^{18}F]fluoride was resolubilized into 300 μL of anhydrous acetonitrile and transferred to a Reactivial precharged with ethylene glycol bistriflate (2 mg, 6.2 μmol) in 100 μL of anhydrous acetonitrile. The container was capped tightly, and the mixture was heated at 110 $^\circ\text{C}$ for 2 min and then cooled to 0 $^\circ\text{C}$ in an ice bath. Triflic anhydride (5 μL) was added to the reaction solution, and this mixture was allowed to incubate for 3 min at room temperature. To remove unreacted [^{18}F]fluoride, the solution was passed through a short alumina plug (1 cm in a Pasteur pipet), which was eluted with 2×300 μL of anhydrous acetonitrile. The eluant (containing [^{18}F]fluoroethyl triflate) was transferred to a Reactivial containing 2 mg of thiourea in 100 μL of DMF. The resulting mixture in the capped vial was heated at 110 $^\circ\text{C}$. After 30 min, the reaction mixture was removed from the oil bath and the organic solvent (acetonitrile) was evaporated under a stream of nitrogen. The residue was taken up in 2 mL of HPLC solvent and purified on a Whatman SCX semipreparative HPLC column eluted

isocratically with a solvent of 5% ethanol in 0.15 N saline at a flow rate of 5 mL/min. The desired product **3b**, retention time 14.5 min, was collected for further study. The total reaction and purification time was 110 min; decay-corrected radiochemical yield was between 4.5% and 10%. The radiochemical purity of **3b** was analyzed by an analytical SCX HPLC column (eluted isocratically with a solvent of 5% acetonitrile in 0.05 N saline at a flow rate of 2 mL/min) and found to be greater than 98%. By comparison of the integrated sample UV signal with a calibrated compound **3a** mass/UV absorbance curve, specific activity was determined to be 120–300 Ci/mmol at the end of synthesis. The identity of the tracer was confirmed by the coelution of **3b** with nonradioactive standard **3a** on the analytical HPLC system.

Radiochemical Synthesis of [¹⁴C]Methylisothiourea Chloride (1b). [¹⁴C]Methyl iodide was prepared using a previously reported method.⁵⁵ Carbon-11 was produced by an ¹⁴N(p,α)¹¹C nuclear reaction, converted to ¹¹CO₂ in the target of 0.5% O₂/99.5% N₂, and then trapped under vacuum in a copper coil cooled with liquid nitrogen. The trap was warmed to room temperature, and the ¹¹CO₂ was bubbled through 0.1 mL of LiAlH₄ in ether (1.0 M) for 3–5 min. The ether was evaporated by bubbling nitrogen through the solution. After the aqueous HI (57%, 3 mL) was added, the mixture was heated to 100 °C for 5 min. The [¹⁴C]methyl iodide formed was distilled through a drying tube filled with NaOH pellets and P₂O₅ powder and then trapped at 0 °C in a 2 mL conical vial containing 1 mL of acetone. The collected [¹⁴C]methyl iodide activity was transferred to a Reactivial with 2 mg of thiourea. The mixture was refluxed at 110 °C for 6 min. The residue was dissolved in 2 mL of HPLC solvent and purified on a Whatman SCX semipreparative HPLC column eluted isocratically with solvent of 0.1 N saline at a flow rate of 5 mL/min. The desired product **1b**, retention time 19.2 min, was collected for further study. The total reaction and purification time was 50 min, and decay-corrected radiochemical yield ranged from 50% to 80%. The radiochemical purity of **1b** was determined by analytical SCX HPLC (eluted isocratically with solvent of 5% acetonitrile in 0.05 N saline at a flow rate of 2 mL/min) to be greater than 99%. By comparison of the integrated sample UV signal with a calibrated compound **1a** mass/UV absorbance curve, specific activity was determined to be greater than 500 Ci/mmol at the end of synthesis. The identity of the tracer was confirmed by the coelution of **1b** with nonradioactive standard on the analytical HPLC system.

Determination of Partition Coefficients (log P_{ow}). Partition coefficients for **3b** and **1b** were measured at pH 6.8 as follows. A 1–20 μCi sample of radiolabeled compound with volume less than 50 μL in 2.5% EtOH/0.05 N saline was added to a premixed suspension of 1 mL of octanol in 1 mL of water. The resulting solution was mixed for 30–45 s and centrifuged for 5 min at 2000 rpm. An 800 μL aliquot of the octanol layer was removed and extracted with 800 μL of water. The solution was mixed and centrifuged as before. A 500 μL aliquot of the octanol layer was removed and extracted with 500 μL of water. The radioactivity of each layer of the back-extraction was measured. Each octanol and water layer was weighed. The partition coefficient was calculated as the ratio of cpm/g of octanol to cpm/g of water per extraction. Experiments were conducted in quadruplicate. The average log P_{ow} value of the three back-extractions for the four trials is reported.

iNOS Induction in J774 Macrophages. The mouse macrophage cell line J774 was obtained from Monsanto Co. and grown at 37 °C, 5% CO₂, in Dulbecco's modified Eagle's medium (DMEM) supplemented with 10% fetal calf serum and 2 mM glutamine. Cells were cultured in 75 cm² flasks (20 mL/flask) until they reached confluence. Induction of iNOS was initiated by adding fresh media containing *Escherichia coli* lipopolysaccharide (1 μg/mL; stereotype 0111:B4) with or without γ-interferon (120 units/mL). Incubation was terminated at predetermined time points (2, 4, 6, 8, 12, 24 h). Cells were rinsed twice with ice cold PBS and lysed in 4 mL of modified NP-40 lysis (0.5% NP-40, 100 mM NaCl, 20 mM Tris, 1 mM EDTA, 10 μg/mL aprotinin, 0.5 mM phenylmethanesulfonyl fluoride, 10 μg/mL leupeptin hemisulfate, pH 8.0) at 0 °C for 30 min. The lysed cells were collected in 10 mL vials

and centrifuged at 10000g for 10 min at 4 °C. Supernatant was collected and centrifuged again at 100000g for 30 min at 4 °C to isolate the cytosolic protein. Protein concentrations of each sample were measured by the BCA assay using bovine serum albumin as a standard.

Western Blot Analysis. Optimum iNOS induction time was assessed by Western blotting. Cytosolic proteins, 100 μg, were boiled with sample treatment buffer (0.125 M Tris, 4% SDS, 20% glycerol, 10% 2-mercaptoethanol, 0.1% bromophenol blue, pH 6.8) for 5 min before loading on 7% SDS-polyacrylamide gels. After electrophoresis, proteins were transferred to nitrocellulose sheets in transfer buffer (0.76 M glycine, 20% methanol, 2.5 mM Tris, pH 8) using a blotting apparatus for 4 h at 4 °C. The blot was blocked in TBST buffer (10 mM Tris, 0.15 M NaCl, 0.05% Tween 20, pH 8.0) and 10% bovine milk powder for 1 h at room temperature and then incubated with anti-iNOS mouse monoclonal antibody (1:150 dilution; Signal Transduction Inc.) overnight at 4 °C. The blot was washed four times with TBST buffer (10 min each) followed by incubation with goat anti-mouse antibody conjugated to alkaline phosphatase for 1 h at room temperature. The blot was washed again in TBST buffer (4 × 10 min), and the specific immune complexes were revealed by incubation with 5-bromo-4-chloro-3-indoylphosphate *p*-toluidine and nitroblue tetrazolium (Sigma). Prestained blue protein (Sigma) markers were used for molecular weight determinations.

Cell Uptake Study. J774 cells were plated in 6-well plates and grown to confluence in DMEM medium supplemented with 10% fetal calf serum and 2 mM glutamine. Cells were divided into three groups: control, pretreated, and blocking group (*n* = 4/group/time point). iNOS was induced in the pretreated group as well as the blocking group with DMEM containing LPS and γ-interferon using the above conditions. The control group was treated with DMEM only. Cells were rinsed twice with a modified HEPES-buffered Krebs solution (131 mM NaCl, 5.5 mM KCl, 1 mM MgCl₂, 2.5 mM CaCl₂, 25 mM NaHCO₃, 1 mM NaH₂PO₄, 5.5 mM D-glucose, 20 mM HEPES, pH 7.4)⁴² maintained at 37 °C. Tracer uptake was initiated by adding loading buffer, HEPES-buffered Krebs (2 mL/well, 37 °C) containing either **3b** (1–2 μCi/mL) or **1b** (15–30 μCi/mL), to the monolayers. For the blocking group, the loading buffer contained an additional 0.1 mM ethylisothiourenium hydrochloride as a blocking agent. Incubation was terminated at various times by removing the loading buffer from plates. The monolayers were washed with 2 mL of ice cold PBS solution three times to clear extracellular spaces and extracted in 2 mL of a 1% (w/v) sodium dodecyl sulfate/10 mM sodium borate solution. A sample of the loading buffer (0.1 mL) from each well was collected into a 1 mL hinged-cap centrifuge tube (Eppendorf) for standardizing cellular data with extracellular tracer concentration (nM_o). Cell extracts (1 mL) and the loading buffer samples were counted for radioactivity in an automatic well-type gamma counter (Gamma 8000, Beckman). Cell samples were then quantified for protein content by BCA assay, using bovine serum albumin as the protein standard. The uptake data are presented as fmol·(mg of protein)⁻¹·(nM_o)⁻¹.

Serum Stability Study. *In vivo* and *in vitro* stability studies for both **3b** and **1b** were performed. In the *in vivo* experiments, the radiotracer was injected into the tail vein of the anesthetized rats. Blood samples were obtained via cardiac puncture at various time points postinjection and centrifuged for 2 min at 14 000 rpm. The plasma was separated from the red blood cell pellet and analyzed by HPLC with the semipreparative SCX column. HPLC fractions were collected and counted on an automatic well-type gamma counter (Gamma 8000, Beckman). Radioactivity balance was determined by comparing injected activity with total activity eluted from the column. The *in vitro* studies were carried out by adding the radiotracer (dissolved in 0.3 mL of 0.1 N NaCl) to 3 mL of fresh rat blood. The mixture was incubated at 37 °C and 100 μL aliquot samples were withdrawn at specific time points for analysis as described above.

Biodistribution Studies. The biodistribution studies were performed in mature female Sprague–Dawley rats (150–200 g). Radiolabeled tracer, **3b** or **1b** in saline solution, was

administered to the rats under Metaflane anesthesia via tail vein injection. The animals were allowed free access to water and food. At specific time points post-tracer administration, the rats were reanesthetized and sacrificed by decapitation. The organs/tissues of interest were removed and weighed. The radioactivity levels in the sampled organs/tissues were determined using an automatic well-type gamma counter (Gamma 8000, Beckman). The percent injected dose per gram of tissue (%ID/g) was calculated by comparison to a weighed and counted standard solution of the injectate.

Pretreatment Studies. Three groups of mature female Sprague–Dawley rats ($n = 4$) were used in the experiments: control, pretreatment, and blocking group. iNOS was induced in the pretreatment group as well as the blocking group by intravenous injection of 15 mg/kg LPS (in saline) 6 h (if not specified) before the tracer administration. The control group was injected with saline only 6 h before tracer administration. For the blocking group, an additional 10 mg/kg *S*-ethylisothiourea was coinjected with tracer as a blocking agent. The biodistribution of each tracer in both groups was determined as described above. The Student's *t*-test was employed to analyze all statistical data.

Acknowledgment. The authors would like to thank Dr. Vallabhaneni V. Rao for his help in Western blot experiments, Carmen S. Dence for assistance in $^{11}\text{CH}_3\text{I}$ production, and Elizabeth L. C. Sherman and Michael Cristel for their support in the animal and cell studies. In addition, special thanks go to Joanna B. Downer and Teresa M. Jones-Wilson for excellent editorial assistance and helpful discussions. This work was supported by grants from the National Institutes of Health (NIH P01-HL-13851 to M.J.W.) and the Monsanto/Washington University Biomedical Agreement.

Supporting Information Available: Detailed biodistribution data for **3b** (at 10 and 30 min) and **1b** (at 30 min) in LPS-pretreated as well as control mature female Sprague–Dawley rats (2 pages). Ordering information is given on any current masthead page.

References

- Zhang, J.; McCarthy, T. J.; Moore, W. M.; Jerome, G. M.; Currie, M. G.; Welch, M. J. Nitric oxide synthase (NOS) inhibitors for PET: synthesis, evaluation and radiolabeling of potential NOS radiotracers. *J. Nucl. Med.* **1995**, *36*, 48P.
- Moncada, S.; Palmer, R. M. J.; Higgs, E. A. Nitric oxide: Physiology, pathophysiology, and pharmacology. *Pharmacol. Rev.* **1991**, *43*, 109–142.
- Nathan, C. F. Nitric oxide as a secretory product of mammalian cells. *FASEB* **1992**, *6*, 3051–3064.
- Stuehr, D. J.; Griffith, O. W. Mammalian nitric oxide synthases. *Adv. Enzymol. Rel. Mol. Biol.* **1992**, *65*, 287–346.
- Marletta, M. A. Nitric oxide synthase structure and mechanism. *J. Biol. Chem.* **1993**, *268*, 12231–12234.
- Förstermann, U.; Closs, E.; Pollock, J. S.; Nakane, M.; Schwarz, P.; Gath, I.; Kleinert, H. Nitric oxide synthase isozymes characterization, purification, molecular cloning, and functions. *Hypertension* **1994**, *23*, 1121–1131.
- Moncada, S.; Higgs, A. The L-arginine-nitric oxide pathway. *New Engl. J. Med.* **1993**, *329*, 2002–2012.
- Kerwin, J. F. K., Jr.; Heller, M. The arginine-nitric oxide pathway: a target for new drugs. *Med. Res. Rev.* **1994**, *14*, 23–74.
- Kerwin, J. F. K., Jr.; Lancaster, J. R., Jr.; Feldman, P. L. Nitric oxide: a new paradigm for second messengers. *J. Med. Chem.* **1995**, *38*, 4343–4362.
- Kilbourn, R. G.; Jubran, A.; Gross, S. S.; Griffith, O. W.; Levi, R.; Adams, J.; Lodato, R. F. Reversal of endotoxin-mediated shock by N^G -methyl-L-arginine, an inhibitor of nitric oxide synthesis. *Biochem. Biophys. Res. Commun.* **1990**, *172*, 1132–1138.
- Petros, A.; Vallance, P. Nitric oxide synthase inhibitors in human septic shock. In *Nitric Oxide: Brain and Immune System*; Moncada, S., Nisticò, G., Higgs, E. A., Eds.; Portland Press: London, 1993; pp 259–264.
- Ter-Pogossian, M. M.; Raichle, M. E.; Sobel, B. E. Positron emission tomography. *Sci. Am.* **1980**, *243*, 170–181.
- Fowler, J. S. Positron Emitter Labeled Enzyme Inhibitors and Substrates. In *Radiopharmaceuticals: Chemistry and Pharmacology*; Nunn, A. D., Ed.; Marcel Dekker, Inc.: New York, 1992; pp 267–296.
- Hwang, D. R.; Eckelman, W. C.; Mathias, C. J.; Petrillo, E. W.; Lloyd, J.; Welch, M. J. Positron-labeled angiotensin-converting enzyme (ACE) inhibitor: Fluorine-18-fluorocaptopril. Probing the ACE activity *in vivo* by positron emission tomography. *J. Nucl. Med.* **1991**, *32*, 1730–1737.
- Inoue, O.; Tominaga, T.; Yamasaki, T.; Kinemuchi, H. A selective radiotracer for *in vivo* measurement of monoamine oxidase-B activity in the brain. *J. Neurochem.* **1985**, *44*, 210–216.
- Shinotoh, H.; Inoue, O.; Suzuki, K.; Yamasaki, T.; Iyo, M.; Hashimoto, K.; Tominaga, T.; Itoh, T.; Teteno, Y.; Ikehira, H. Kinetics of [^{11}C]N,N-dimethylamine in mice and humans: Potential for the measurement of brain MAO-B activity. *J. Nucl. Med.* **1987**, *28*, 1006–1011.
- Fowler, J. S.; MacGregor, R. R.; Wolf, A. P.; Arnett, C. D.; Dewey, S. L.; Schlyer, D.; Christman, D.; Logan, J.; Smith, M.; Sachs, H.; Aquilonius, S. M.; Bjurling, P.; Hallidin, C. G.; Långström, B. Mapping human brain monoamine oxidase A and B with ^{11}C -suicide inactivators and positron emission tomography. *Science* **1987**, *235*, 481–485.
- Gjedde, A.; Reith, J.; Dyve, S.; Leger, G.; Guttman, M.; Diksic, M.; Evans, A.; Kuwabara, H. Dopa decarboxylase activity of the living human brain. *Proc. Natl. Acad. Sci. U.S.A.* **1991**, *88*, 2721–2725.
- Eckelman, W. C., Ed. *Receptor-Binding Radiotracers*; CRC Press, Inc.: Boca Raton, FL, 1982; Vol. I, II.
- McCarthy, T. J.; Welch, M. J. *In vivo* rat biodistribution of no-carrier-added [I-125]diphenylethiodonium bisulfate. A probe for nitric oxide synthase. *J. Nucl. Med.* **1993**, *34*, 89P.
- Roeda, D.; Crouzel, C.; Brouillet, E.; Valette, H. Synthesis and *in vivo* distribution of no-carrier-added N(ω)-nitro-L-arginine [^{11}C]methyl ester, a nitric oxide synthase inhibitor. *Nucl. Med. Biol.* **1996**, *23*, 509–512.
- Garvey, E. P.; Oplinger, J. A.; Tanourey, G. J.; Sherman, P. A.; Fowler, M.; Marshall, S.; Harmon, M. F.; Paith, J. E.; Furfine, E. S. Potent and selective inhibition of human nitric oxide synthases. Inhibition by non-amino acid isothioureas. *J. Biol. Chem.* **1994**, *269*, 26669–26676.
- Nakane, M.; Klinghofer, V.; Kuk, J. E.; Donnelly, J. L.; Budzik, G. P.; Pollack, J. S.; Basha, F.; Carter, G. W. Novel potent and selective inhibitors of inducible nitric oxide synthase. *Mol. Pharmacol.* **1995**, *47*, 831–834.
- Southan, G. J.; Szabó, C.; Thiemermann, C. Isothioureas: potent inhibitors of nitric oxide synthases with variable isoform selectivity. *Br. J. Pharmacol.* **1995**, *114*, 510–516.
- Eckelman, W. C.; Gibson, R. E. The design of site-directed radiopharmaceuticals for use in drug discovery. In *Nuclear imaging in drug discovery, development, and approval*; Burns, H. D., Gibson, R. E., Dannals, R. F., Siegl, P. K. S., Eds.; Birkhäuser: Boston, 1993; pp 113–134.
- Evans, T.; Carpenter, A.; Cohen, J. Purification of a distinctive form of endotoxin-induced nitric oxide synthase from rat liver. *Proc. Natl. Acad. Sci. U.S.A.* **1992**, *89*, 5361–5365.
- Szabó, C.; Southan, G. J.; Thiemermann, C. Beneficial effects and improved survival in rodent models of septic shock with *S*-methylisothiourea sulfate, a potent and selective inhibitor of inducible nitric oxide synthase. *Proc. Natl. Acad. Sci. U.S.A.* **1994**, *91*, 12472–12476.
- Misko, T. P.; Moore, W. M.; Kasten, T. P.; Nickols, G. A.; Corbett, J. A.; Tilton, R. G.; McDaniel, M. L.; Williamson, J. R.; Currie, M. G. Selective inhibition of the inducible nitric oxide synthase by aminoguanidine. *Eur. J. Pharmacol.* **1993**, *233*, 119–125.
- Moore, W. M.; Webber, R. K.; Jerome, G. M.; Tjoeng, F. S.; Misko, T. P.; Currie, M. G. L- N^6 -(1-iminoethyl)lysine: a selective inhibitor of inducible nitric oxide synthase. *J. Med. Chem.* **1994**, *37*, 3886–3888.
- Olken, N. M.; Marletta, M. A. N^G -allyl and N^G -cyclopropyl-L-arginine: Two novel inhibitors of macrophage nitric oxide synthase. *J. Med. Chem.* **1992**, *35*, 1137–1144.
- Kiesewetter, D. O.; Brücke, T.; Finn, R. D. Radiochemical synthesis of [^{18}F]fluorocaptopril. *Appl. Radiat. Isot.* **1989**, *40*, 455–460.
- Kiesewetter, D.; Finn, R. [^{18}F]Fluoroethyl triflate: Preparation and Reactions with Amines. *J. Labelled Compds. Radiopharm.* **1989**, *26*, 14–15.
- Kiesewetter, D. O.; Kawai, R.; Chelliah, M.; Owens, E.; McLellan, C.; Blasberg, R. G. Preparation and biological evaluation of ^{18}F -labeled benzamide analogs as potential dopamine D_2 receptor ligands. *Nucl. Med. Biol.* **1990**, *17*, 347–356.
- Chi, D. Y.; Kilbourn, M. R.; Katzenellenbogen, J. A.; Brodack, J. W.; Welch, M. J. Synthesis of no-carrier-added N-([^{18}F]fluoroalkyl)piperone derivatives. *Appl. Radiat. Isot.* **1986**, *37*, 1173–1180.

- (35) Suehiro, M.; Wilson, A. A.; Scheffel, U.; Dannals, R. F.; Ravert, H. T.; Wagner, H. N. J. Radiosynthesis and evaluation of N-(3-[¹⁸F]fluoropropyl)paroxetine as a radiotracer for *in vivo* labeling of serotonin uptake site by PET. *Nucl. Med. Biol.* **1991**, *18*, 791–796.
- (36) Zijlstra, S.; Visser, G. M.; Korf, J.; Vaalburg, W. Synthesis and *in vivo* distribution in the rat of several fluorine-18 labeled N-fluoroalkylaporphines. *Appl. Radiat. Isot.* **1993**, *44*, 651–658.
- (37) Nakane, M.; Klinghofer, V.; Kuk, J. E.; Donnelly, J. L.; Budzik, G. P.; Pollock, J. S.; Basha, F.; Carter, G. W. Novel potent and selective inhibitors of inducible nitric oxide synthase. *Mol. Pharmacol.* **1995**, *47*, 831–834.
- (38) Knowles, R. G.; Merrett, M.; Salter, M.; Moncada, S. Differential induction of brain, lung and liver nitric oxide synthase by endotoxin in the rat. *Biochem. J.* **1990**, *270*, 833–836.
- (39) Rosa, M. D.; Radomski, M.; Carnuccio, R.; Moncada, S. Glucocorticoids inhibit the induction of nitric oxide synthase in macrophages. *Biochem. Biophys. Res. Commun.* **1990**, *172*, 1246–1252.
- (40) Xie, Q.; Cho, H. J.; Calaycay, J.; Mumford, R. A.; Swiderek, K. M.; Lee, T. D.; Ding, A.; Troso, T.; Nathan, C. Cloning and characterization of inducible nitric oxide synthase from mouse macrophages. *Science* **1992**, *256*, 225–228.
- (41) Rojas, A.; Delgado, R.; Galaria, L.; Palacios, M. Monocyte chemoattractant protein-1 inhibits the induction of nitric oxide synthase in J774 cells. *Biochem. Biophys. Res. Commun.* **1993**, *196*, 274–279.
- (42) Baydoun, A. R.; Mann, G. E. Selective targeting of nitric oxide synthase inhibitors to system γ^+ in activated macrophages. *Biochem. Biophys. Res. Commun.* **1994**, *200*, 726–731.
- (43) Bogle, R. G.; MacAllister, R. J.; Whitley, G. S. J.; Vallance, P. Induction of N^G-monomethyl-L-arginine uptake: a mechanism for differential inhibition of NO synthases. *Am. J. Physiol.* **1995**, *269*, C750–C756.
- (44) March, J. *Advanced organic chemistry: Reaction, mechanism, and structure*, 4th ed.; John Wiley & Sons: New York, 1992.
- (45) Poss, M. A.; Iwanowicz, E.; Reid, J. A.; Lin, J.; Gu, Z. A mild and efficient method for the preparation of guanidines. *Tetrahedron Lett.* **1992**, *33*, 5933–5936.
- (46) Kim, K. S.; Qian, L. Improved methods for the preparation of guanidines. *Tetrahedron Lett.* **1993**, *34*, 7677–7680.
- (47) Welch, M. J.; Kilbourn, M. R.; Mathias, C. J.; Mintun, M. A.; Raichle, M. E. Comparison in animal models of ¹⁸F-spiroperidol and ¹⁸F-haloperidol: potential agents for imaging the dopamine receptor. *Life Sci.* **1983**, *33*, 1687–1693.
- (48) Perlmutter, J. S.; Kilbourn, M. R.; Raichle, M. E.; Welch, M. J. MPTP-induced upregulation of *in vivo* dopaminergic radioligand-receptor binding in humans. *Neurology* **1987**, *37*, 1575–1579.
- (49) Grubb, R. L. J.; Raichle, M. E.; Higgins, C. S.; Eichling, J. O. Measurement of regional cerebral blood volume by emission tomography. *Ann. Neurol.* **1978**, *4*, 322–328.
- (50) Hom, G. J.; Grant, S. K.; Wolfe, F.; Bach, T. J.; Macintyre, D. E.; Hutchinson, N. I. Lipopolysaccharide-induced hypotension and vascular hyporeactivity in the rat: Tissue analysis of nitric oxide synthase mRNA and protein expression in the presence and absence of dexamethasone, N^G-monomethyl-L-arginine or indomethacin. *J. Pharmacol. Exp. Ther.* **1995**, *272*, 452–459.
- (51) Buttery, L. D. K.; Evans, T. J.; Springall, D. R.; Carpenter, A.; Cohen, J.; Polak, J. M. Immunohistochemical localization of inducible nitric oxide synthase in endotoxin-treated rats. *Lab. Invest.* **1994**, *71*, 755–764.
- (52) Smirk, F. H. Preliminary note on the properties of s-methyl isothiurea sulphate. *Br. Med. J.* **1941**, 510–511.
- (53) Fastier, F. H.; Smirk, F. N. The circulatory effects of some isothiurea derivatives, with special reference to the sensitization of animals to the pressor action of adrenaline. *J. Physiol.* **1943**, *101*, 379–388.
- (54) Kilbourn, M. R.; Jerabek, P. A.; Welch, M. J. An improved [¹⁸O] water target for [¹⁸F] fluoride production. *Appl. Radiat. Isot.* **1985**, *36*, 327–328.
- (55) Buckman, B. O.; VanBrocklin, H. F.; Dence, C. S.; Bergman, S. R.; Welch, M. J.; Katzenellenbogen, J. A. Synthesis and tissue biodistribution of [ω -¹¹C] palmitic acid. A novel PET imaging agent for cardiac fatty acid metabolism. *J. Med. Chem.* **1994**, *37*, 2481–2485.

JM960481Q